Iranian Hydraulic Association
Journal of Hydraulics

Research Article
https://doi.org

Mitigating Local Scour Around Square Bridge Piers Using Novel Interlocking Three-Dimensional Porous Blocks

Aryan Nikmehr[1], Seyed Amin Asghari Pari[2*], and Lotfolah Emadali[3]

[1]MSc., Department of Civil Engineering, Faculty of Engineering, Behbahan Khatam Alanbia University of Technology, Behbahan, Iran.

[1]Associate Professor, Department of Civil Engineering, Faculty of Engineering, Behbahan Khatam Alanbia University of Technology, Behbahan, Iran.

[1] Assistant professor, Department of Civil Engineering, Faculty of Engineering, Behbahan Khatam Alanbia University of Technology, Behbahan, Iran.

*** asghari_amin@bkatu.ac.ir**

Abstract

Local scour around bridge piers remains one of the primary causes of bridge failures worldwide. Conventional countermeasures such as riprap and collars often suffer from stability issues and edge failure under high-velocity flows. This study introduces a novel countermeasure using Interlocking 3D Porous Blocks (IPBs) to protect the sediment bed around square bridge piers. Experimental investigations were conducted in a laboratory flume under clear-water conditions. The effects of the number of block rows (initially 1–4) and vertical placement level (on-bed, semi-buried, and fully buried) were systematically examined. Based on the superior performance of the buried configuration, two additional five-row arrangements (a single buried layer and a double-stacked buried layer) were tested to identify the optimal design. Results demonstrated that the buried configurations significantly outperformed others. The optimal configuration, consisting of the double-stacked, 5-row buried layer, resulted in no measurable scour within the accuracy of the adopted measurement system (±1 mm). This design effectively dissipates the energy of the downflow and horseshoe vortex while maintaining bed integrity. The mechanical interlocking system provided excellent structural integrity, making IPBs a highly promising solution for bridge foundation protection. Field-scale validation is recommended for practical implementation.

Keywords: Local scour; Bridge pier; Hydraulic structure; Interlocking porous blocks; Bed protection.

1. Introduction

Bridges serve as critical nodes in transportation networks, facilitating economic growth and societal connectivity. However, they are frequently exposed to harsh hydraulic conditions, particularly during flood events. Indeed, the vulnerability of these structures is well-documented; statistical analyses from the United States show that hydraulic factors (specifically stream instability and scour) account for approximately 60% of bridge failures (Lagasse et al., 1995; Richardson & Davis, 1995). Similarly, historical data from New Zealand suggests that millions of dollars are spent annually on scour-related repairs (Macky, 1990). The localized lowering of the riverbed around bridge foundations, known as local scour, compromises the foundation's integrity, potentially leading to catastrophic collapse and loss of life (Miller, 2003). Therefore, the development of efficient, durable, and cost-effective countermeasures to mitigate local scour remains a paramount challenge in hydraulic engineering.

The mechanism of local scour is primarily driven by the interference of the pier with the approaching flow. When the flow encounters a pier, it decelerates, creating a stagnation pressure gradient that drives the flow downwards at the upstream face. This "down-flow" acts like a vertical jet, eroding the bed material at the pier base. Simultaneously, the separated flow rolls up to form the "horseshoe vortex" system, which entrains and transports the eroded sediment downstream (Raudkivi & Ettema, 1983; Melville & Coleman, 2000). The intensity of these vortices is strongly influenced by pier geometry; notably, square piers (often used in older bridges or specific construction methods) induce stronger horseshoe vortices and deeper scour holes compared to circular piers due to pronounced flow separation at their sharp corners. This makes them a critical benchmark for evaluating countermeasure effectiveness.

Over the past decades, numerous countermeasures have been proposed to combat this phenomenon, generally categorized into two groups: flow-altering devices and bed-armoring countermeasures. Flow-altering devices, such as sacrificial piles (Melville & Hadfield, 1999), collars (Zarrati et al., 2004; Moncada-M et al., 2009), and slots (Kumar et al., 1999), aim to weaken the down-flow or divert the horseshoe vortex. While these methods can be effective, they often face practical limitations. For example, slots may compromise the structural capacity of the pier or become clogged with floating debris, and collars may lose efficiency if the bed level degrades generally (general scour) below the collar placement.

Consequently, bed-armoring remains the most widely adopted strategy. Riprap (loose rock dumping) is the industry standard due to its availability and ease of installation (Chiew, 2004). However, riprap is prone to several failure modes, including shear failure under high-velocity flows, winnowing of fine bed material through the voids between stones, and edge failure at the periphery of the protected area (Lauchlan & Melville, 2001). To address the inherent instability of loose elements, recent research has focused on Articulated Concrete Blocks (ACBs) and complex artificial elements like A-Jacks. Studies by Zolghadr and Shafai-Bajestan (2018) and Valela et al. (2022) have demonstrated that elements with high interlocking capacity and specific geometries can outperform traditional riprap. These elements work not just by shielding the bed, but also by increasing hydraulic roughness and dissipating turbulent energy.

Despite these advancements, comprehensive reviews (e.g., Behera et al., 2026) highlight that even robust systems like riprap and articulated blocks face challenges with edge failure, installation, or material intensity. This underscores an ongoing search for an integrated

countermeasure that combines mechanical interlocking, hydraulic energy dissipation, and structural integrity. The ideal solution should be both porous (to dissipate vortex energy) and interlocking, to form a coherent mat that resists failure. The ideal countermeasure should be both porous (to relieve uplift pressure and dissipate vortex energy within its matrix) and interlocking, to act as a coherent, flexible mat rather than as individual loose units. This study addresses this need by introducing and experimentally evaluating a novel countermeasure: the Interlocking 3D Porous Block (IPB). While similar porous elements have been utilized in other hydraulic applications, such as energy dissipation in stilling basins, their application for mitigating bridge pier scour has not been extensively explored. The IPB distinguishes itself with a cubic lattice design that promotes multi-directional flow passage and internal energy dissipation, while its mechanical interlocking mechanism ensures stability against the hostile flow field around the pier.

The primary objective of this research is to investigate the efficiency of IPBs in reducing local scour around a square pier under clear-water conditions. A key contribution of this work is the systematic evaluation of the critical interplay between the protection's areal extent (number of rows) and its vertical placement level (on-bed, semi-buried, and fully buried), a parameter often overlooked in bed armoring studies but found here to be decisive. By analyzing the equilibrium scour depth and the time-evolution of the scour hole, this study aims to offer preliminary recommendations on the effective placement of 3D porous blocks for their use as a sustainable solution for bridge foundation protection.

2. Materials and Methods

2.1. Experimental Facility

The experiments were conducted in a recirculating rectangular flume at the Hydraulic Research Laboratory of Khatam Alanbia University of Technology. The flume has a 6-m long straight test section with a width of 0.6 m and a depth of 0.6 m. The sidewalls are constructed from tempered glass to facilitate direct visual observation and photographic documentation. To ensure fully developed turbulent flow and minimize entrance effects, the inflow passed through a settling basin equipped with honeycomb screens and a floating damper. A tailgate at the downstream end was used to control the flow depth. Water discharge was supplied by a centrifugal pump and measured using a precise ultrasonic flowmeter (accuracy ±0.1 L/s) installed on the supply line.

2.2. Bed Material and Pier Characteristics

A uniform sand was selected as the bed material to minimize the effects of sediment gradation on scour depth. To prevent the formation of bedforms (ripples) that could interfere with scour measurements, a uniform sand with a median particle size (d_{50}) of 1.2 mm was used. This satisfies the criterion ($d_{50} \geq 0.7$ mm) proposed by Raudkivi and Ettema (1983). The sediment had a geometric standard deviation ($\sigma_g = \sqrt{(d_{84}/d_{16})}$) of approximately 1.25. A square pier with a width (B) of 40 mm was used. This geometry was chosen to represent a "worst-case" scenario for local scour due to strong flow separation at the sharp leading corners. To eliminate sidewall effects, the ratio of flume width to pier width (W/B) was maintained at 15, which is well above the minimum criterion of 6.25 recommended by Chiew and Melville (1987).

2.3. The Novel Countermeasure: Interlocking 3D Porous Blocks (IPBs)

The protective elements used in this study are cubic, interlocking units measuring 20 mm × 20 mm × 20 mm. These blocks, termed Interlocking 3D Porous Blocks (IPBs), were fabricated from a lightweight, high-density polymer using additive

manufacturing (3D printing). The material has a density of approximately 1150 kg/m³ and provides high mechanical strength and durability sufficient to prevent deformation under handling and experimental loading. The blocks feature a lattice structure that yields a nominal porosity of approximately 25% and exhibit a slightly textured surface finish inherent to the manufacturing process.

A key feature of the IPBs is their six-sided mechanical interlocking system. Each face of the cubic block is designed with a system of integrated tongues and grooves. This allows each block to be physically and securely connected to its neighbors in all three dimensions (horizontally, vertically, and transversely). In the experiments, the blocks were manually press-fit together, forming a continuous and coherent, yet flexible, mat. This true mechanical lock distinguishes IPBs from traditional riprap (which relies on gravity) or armor units that are merely placed in an interlocking pattern. The resulting mattress resists shear failure, individual block dislodgement, and edge overturning.

Initial experimental investigations were conducted using 1 to 4 rows of IPBs arranged symmetrically around the pier. For each arrangement, three vertical placement levels were tested: (1) on-bed, (2) semi-buried, and (3) fully buried (with the top surface flush with the bed). As the fully buried configuration yielded the most favorable results, the study was extended to explore optimal five-row arrangements. Two additional configurations were subsequently tested: (1) a five-row single buried layer, and (2) a five-row double-stacked buried layer. All tested configurations are illustrated in Figure 1.

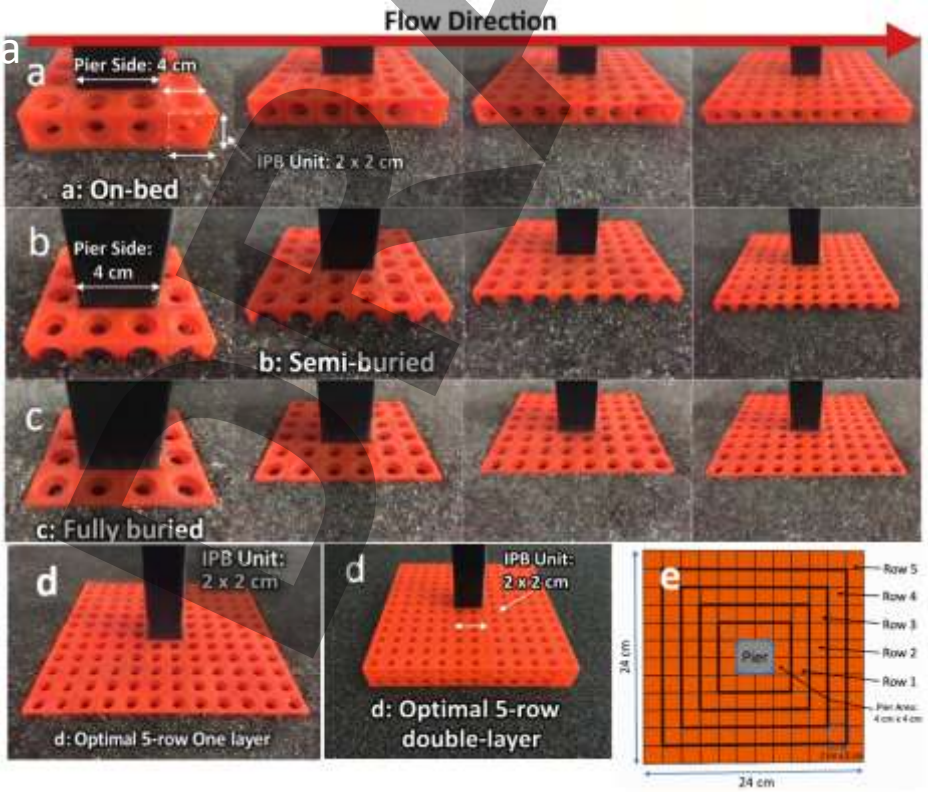

Fig. 1 Experimental configurations of IPBs around the square pier: (a) On-bed placement with 1–4 rows; (b) Semi-buried placement with 1–4 rows; (c) Fully buried placement with 1–4 rows; (d) Optimal 5-row configurations: single-layer and double-layer (stacked) in fully buried position; (e) schematic plan of 5-row configurations.

2.4. Hydraulic Conditions

All experiments were conducted under clear-water scour conditions, where the mean approach flow velocity (U) was kept just below the critical velocity for incipient motion of the bed material (Uc). The critical velocity was determined experimentally by incrementally increasing the flow velocity until general sediment motion was observed, and this value was cross-validated with calculations based on the Shields diagram and the Melville and Sutherland (1988) equation. The flow intensity ratio (U/Uc) was maintained at approximately 0.95 to maximize scour potential without inducing general bed transport, consistent with standard clear-water testing protocols (e.g., Tafarojnoruz et al., 2012).

The flow depth (y) was kept constant at 0.15 m for all experiments, resulting in a flow depth to pier width ratio (y/B) of 3.75. Since local scour depth is largely independent of flow depth for y/B > 3.5 (Melville & Coleman, 2000), this choice effectively eliminates shallow water effects. The key hydraulic and geometric parameters, summarized in Table 1, ensure that the experiments were conducted under subcritical (Fr < 1.0) and fully turbulent flow (Re > 7 × 10^4) conditions, representative of typical field scenarios.

Table 1. Summary of key hydraulic and geometric parameters.

Parameter	Symbol	Value	Criterion/Reference
Flow depth	y	0.15 m	Constant
Pier width	B	40 mm	Constant
Discharge	Q	0.031 m³/s	Measured (±0.1 L/s)
Mean approach velocity	U	0.345 m/s	Calculated
Critical velocity	Uc	0.363 m/s	Shields + Melville & Sutherland (1988)
Flow intensity	U/Uc	0.95	Clear-water condition
Froude number	Fr	0.28	Subcritical
Reynolds number	Re	1.38×10^4	Fully turbulent (> 7×10³)
Flow depth to pier width ratio	y/B	3.75	> 3.5 (Melville & Coleman, 2000)
Flume width to pier width ratio	W/B	15	> 6.25 (Chiew & Melville, 1987)
Median sediment size	d50	1.2 mm	≥ 0.7 mm (Raudkivi & Ettema, 1983)
Sediment geometric std. dev.	σg	1.25	Uniform sediment
Pier width to sediment ratio	B/d50	33.3	> 20 (Melville & Coleman, 2000)
Sediment bed thickness	—	0.25 m	Sufficient to avoid bed effects
Distance of pier from upstream end of recess	—	2.5 m	To ensure fully developed flow

2.5. Dimensional Analysis

Based on the Buckingham π theorem, the dimensionless maximum scour depth and scour hole dimensions can be expressed as:

$$\frac{d_{s\,max}}{B}, \frac{b_s}{B}, \frac{l_s}{B} = f(\mathrm{Re}, \mathrm{Fr}, \frac{y}{B}, \frac{d_{50}}{B}, \frac{U}{U_c}, \alpha, \beta, \gamma, n_p, \phi, B_b/B)$$

where:

- $d_{s\,\max}$ = maximum scour depth,
- b_s, l_s = scour hole width and length,
- Re = Reynolds number, Fr = Froude number,
- y/B = flow depth to pier width ratio,
- B/d_{50} = pier width to median sediment size ratio,
- U/U_c = flow intensity,
- α = number of block rows (areal extent),
- β = vertical placement level (on-bed = 0, semi-buried = 0.5, fully buried = 1.0),
- γ = number of stacked layers,
- n_p = number of porous layers,
- ϕ = porosity (≈ 0.25),
- B_b/B = block-to-pier size ratio (= 0.5).

Since flow and sediment parameters (Re, Fr, U/Uc, y/B, B/d_{50}, ϕ, Bb/B) were kept constant throughout all experiments, the study focused on the functional relationship:

$$\frac{d_{s\,max}}{B}, \frac{b_s}{B}, \frac{l_s}{B} = f(\alpha, \beta, \gamma)$$

2.6. Instrumentation and Procedure

Before each test, the sediment bed was carefully leveled using a carriage-mounted scraper. The IPBs were then installed around the pier according to the specific test scenario. The flume was filled very slowly from the downstream end to ensure the saturation of the bed material without causing any initial disturbance. The duration of each experiment was set to 12 hours. This was based on a preliminary 24-hour control test, which showed that the scour process had reached equilibrium (defined as a scour depth change of less than 1 mm over a 3-hour period, as per Kumar et al., 1999) well within this timeframe. At the end of each test, the flume was carefully drained. The final bed topography was mapped using an automated Bed Profiler equipped with a laser distance sensor. This profiler captured data points on a 10 mm × 10 mm spatial grid with a manufacturer-specified accuracy of ±1.0 mm. For verification, the maximum scour depth was independently measured using a high-precision Leica laser distance sensor (Model: DISTO™ X310). The sensor was operated manually, and its position was guided by a transparent gridded overlay placed on the measurement area. This secondary instrument also has a certified measurement accuracy of ±1.0 mm. To assess experimental reproducibility and establish a robust uncertainty bound, a repeatability analysis was conducted. Five tests were randomly selected from different configurations and repeated under identical conditions... The maximum deviation was ±2 mm, with a mean absolute deviation of 1.0 mm. To assess experimental reproducibility, five tests were randomly selected from different configurations and placement levels and repeated under identical hydraulic conditions. One of these tests (On-bed, 2 rows) was repeated twice, resulting in a total of six repeated runs. The results are presented in Table 2.

Table 2. Results of the repeatability analysis

Test Configuration	Original ds max (cm)	Repeated ds max (cm)	Difference (mm)
On-bed, 2 rows	2.6	2.4	-2
On-bed, 2 rows	2.6	2.7	1
Semi-buried, 4 rows	1.5	1.6	1
Buried, 3 rows	1.7	1.7	0
Buried, 5 rows (single layer)	0.9	1	1
Control (unprotected)	6.8	6.7	-1

The maximum deviation between original and repeated measurements was ±2 mm, with a mean absolute deviation of 1.0 mm across all six runs. These values are consistent with the instrument accuracy of ±1.0 mm and indicate excellent experimental reproducibility. Based on these results, a conservative combined experimental uncertainty of ±2 mm was adopted for all scour depth measurements.

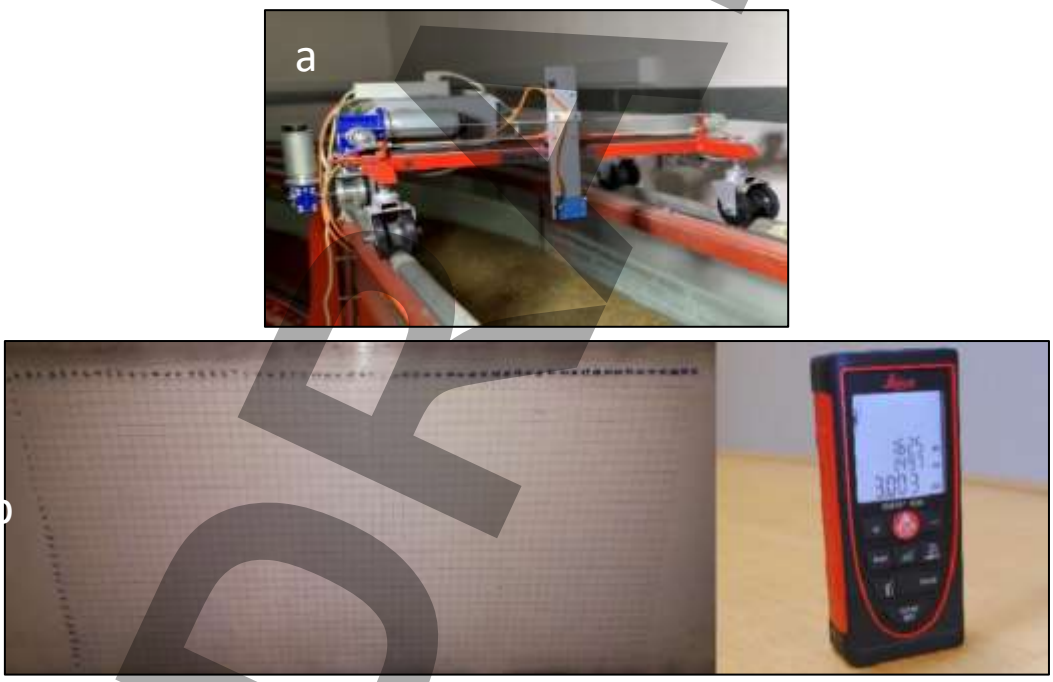

Fig. 2 Measurement instruments: (a) Bed Profiler with integrated laser distance sensor; (b) Leica laser distance sensor and grid plate used for verification and precise scour hole dimensioning.

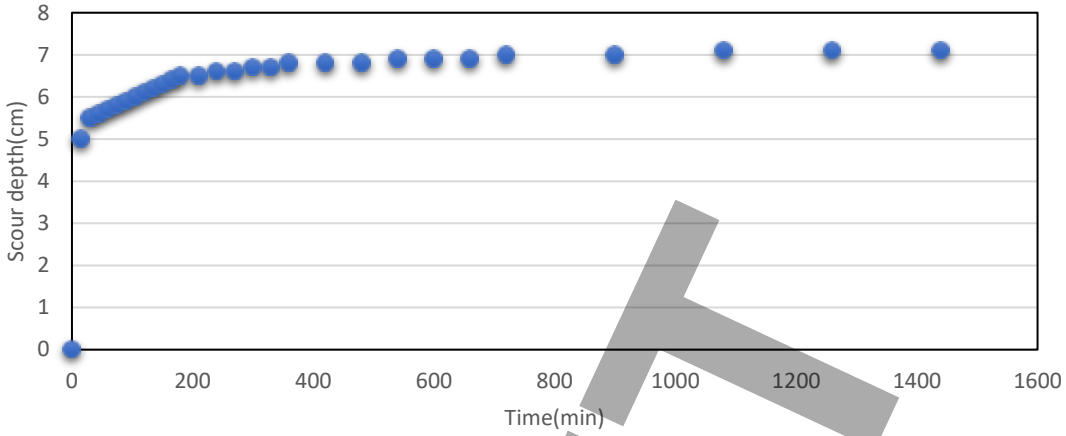

Fig. 3 Time evolution of the maximum scour depth for the unprotected pier (control test), showing the approach to equilibrium.

3. Results

This section presents the experimental results, starting with the baseline control test, followed by a systematic evaluation of the IPB configurations.

3.1 Control Test (Unprotected Pier)

In the absence of any countermeasure, the equilibrium maximum scour depth (ds max) reached 6.8 cm after 12 hours, corresponding to a dimensionless scour depth (ds max/B) of 1.7. The scour hole exhibited a characteristic asymmetric shape, with the deepest erosion occurring at the upstream nose of the pier, driven by the horseshoe vortex. The scour hole width (bs) and length (ls) were 28.0 cm (bs/B = 7.0) and 29.6 cm (ls/B = 7.4), respectively. The temporal evolution of scour depth (Figure 3) showed a rapid initial phase, with over 80% of the final scour occurring within the first 3 hours.

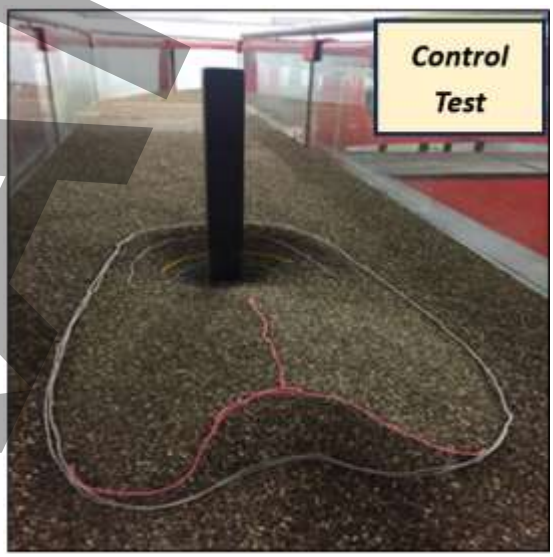

Fig. 4 3D view and contour map of the bed topography for the Control Test (unprotected pier).

3.2 On-Bed Placement (Case A)

Increasing the number of rows progressively reduced scour (Table 3). One row yielded $d_{s\,\max} = 4.3$cm (36.8% reduction). Four rows reduced depth to 1.9 cm (72.1% reduction). Deposition behind the pier formed larger, more symmetric lobes with additional rows. Bed contours (Figure 5a) show contraction of the erosion zone around the pier.

Table 3 Scour Hole Parameters for On-Bed Placement (Case A: Blocks Flush with Bed Surface)

Test Case	ds_{max} (cm)	ds_{max}/B	bs/B	ls/B	Scour Reduction (%)
Control (12 h)	6.8	1.7	7	7.4	—
1 row	4.3	1.08	3.9	3	36.8
2 rows	2.6	0.65	4.7	4.1	61.8
3 rows	2.2	0.55	5.8	5	67.6
4 rows	1.9	0.48	6.9	6.1	72.1

Although the maximum scour depth ($d_{s\,\max}$) decreased monotonically with increasing number of rows, the scour hole planform dimensions (b_s/B and l_s/B) did not necessarily follow a monotonic decreasing trend. With additional rows, the IPB mat increasingly protected the pier vicinity and weakened the horseshoe vortex action at the pier base; consequently, the residual erosion shifted toward the outer boundary of the protection. Since b_s and l_s represent the overall lateral and streamwise extent of the eroded zone, moving the locus of scour outward can yield a broader (larger b_s and l_s) but much shallower depression, i.e., a footprint dominated by edge-related scour rather than a deep pier-adjacent hole.

3.3 Half-Submerged (Semi-Buried) Placement (Case B)

Further improvement was observed (Table 4). One row provided 43% reduction ($d_{s\,\max} = 3.9$ cm). Four rows achieved 78% reduction ($d_{s\,\max} = 1.5$ cm). While $d_{s\,\max}$ decreased with additional rows, b_s/B and l_s/B did not decrease monotonically because the remaining scour progressively migrated to the perimeter of the IPB coverage, producing a broader but shallower edge-related erosion zone. Contours (Figure 5b) indicate narrower and shallower holes, with sediment deposition beginning to fill voids within the block matrix.

3.4 Fully Submerged Below-Bed Placement (Case C)

Sub-bed placement provided the highest single-layer performance (Table 5). One row yielded 54% reduction ($d_{s\,\max} = 3.1$ cm). Four rows achieved 84% reduction ($d_{s\,\max} = 1.1$ cm). Hole geometry was markedly reduced. Contours (Figure 5c) reveal almost complete suppression of upstream erosion. The comparative performance of all three placement levels is clearly visualized in Figure 6, which plots the scour depth reduction against the number of rows.

Table 4. Scour hole parameters around the pier (semi-buried placement)

Test Case	ds_{max} (cm)	ds_{max}/B	bs/B	ls/B	Scour Reduction (%)
Control (12 h)	6.8	1.7	7	7.4	—
1 row	3.9	0.98	3.3	2.8	42.6
2 rows	2.4	0.6	4.4	3.9	64.7
3 rows	2	0.5	5.3	4.7	70.6
4 rows	1.5	0.38	6.4	5.8	77.9

Table 5. Scour Hole Parameters for Fully Buried Placement (Case C)

Test Case	ds_{max}(cm)	ds_{max}/B	bs/B	ls/B	Scour Reduction (%)
Control (12 h)	6.8	1.7	7	7.4	—
1 row	3.1	0.78	2.8	2.5	54.4
2 rows	2.2	0.55	3.9	3.6	67.6
3 rows	1.7	0.43	4.7	4.7	75
4 rows	1.1	0.28	5.8	5.6	83.8

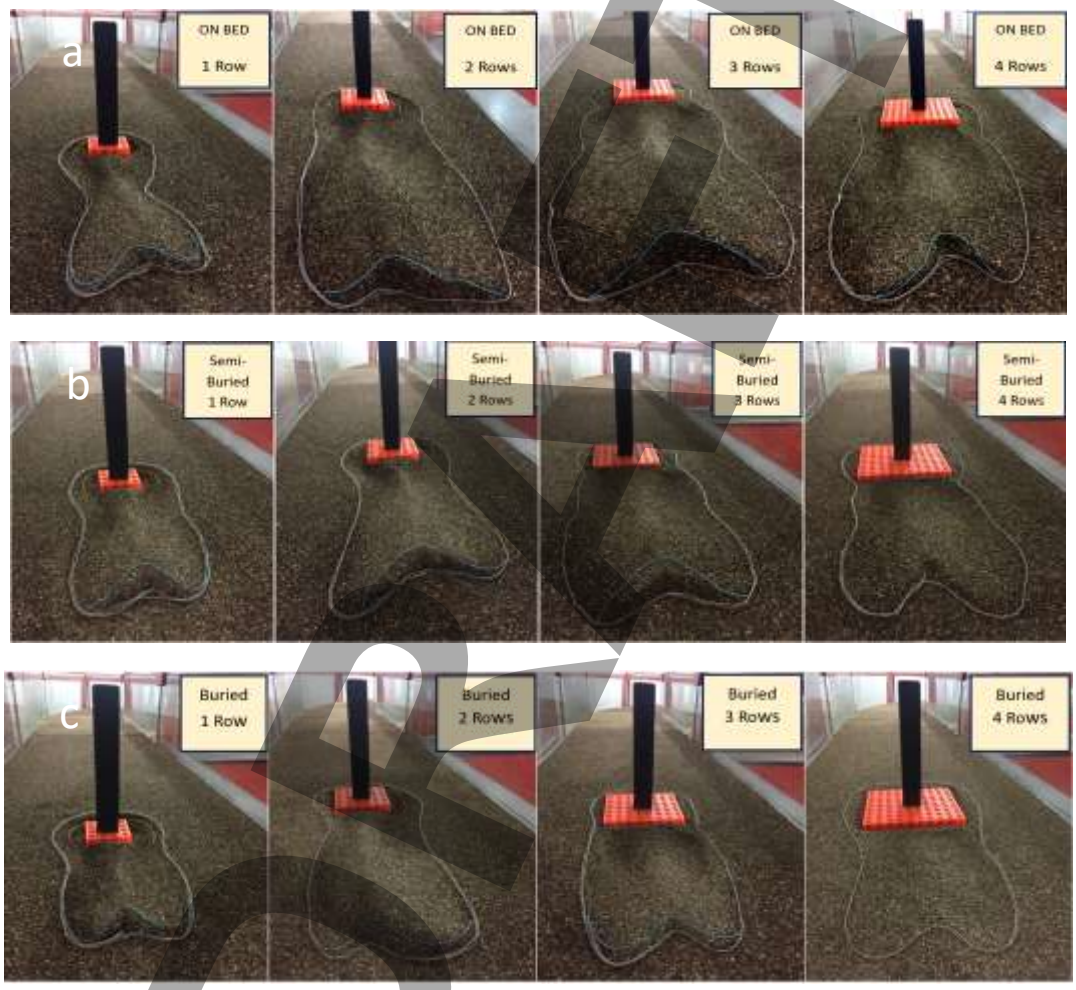

Fig. 5 3D view of the bed topography for (a) on-bed placement (1–4 rows), (b) semi-buried placement (1–4 rows), (c) buried placement (1–4 rows).

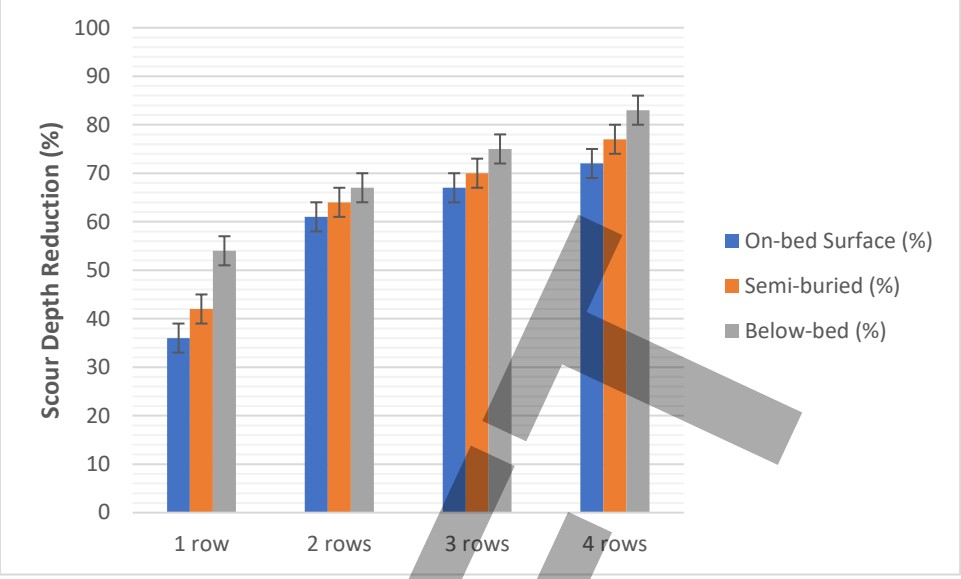

Fig. 6 Comparison of scour depth reduction versus the number of block rows for different placement levels. Error bars represent the combined experimental uncertainty of ±2 mm (approximately ±3% in scour reduction), based on the repeatability analysis (Table 2).

3.5. Effect of Protection Extent (Number of Rows) and Selection of the Optimal Configuration

Figure 6 shows that enlarging the protected area by increasing the number of IPB rows leads to a consistent reduction in the equilibrium maximum scour depth for all three placement levels (on-bed, semi-buried, and fully buried). In addition to lowering $d_{s\,\max}$, increasing the number of rows also constrained the scour hole and displaced the main erosion zone away from the pier, indicating that a wider protection footprint more effectively intercepted the near-bed flow structures responsible for sediment entrainment. The improvement with additional rows was most pronounced for the buried arrangement, which performed best across all row numbers (Tables 2–4). This consistent superiority motivated extending the buried configuration to a 5-row layout to identify the most effective (optimal) setup. Two 5-row buried scenarios were tested: (i) a single-layer mat and (ii) a double-layer (stacked) mat, both installed fully buried with the top surface flush with the initial bed level. The single-layer 5-row configuration reduced scour to $d_{s\,\max} = 0.9$ cm, corresponding to an approximately 91% reduction relative to the control case ($d_{s\,\max} = 6.8$ cm at 12 h). In contrast, the double-layer 5-row configuration produced no measurable local scour within the resolution of the adopted measurement system (±1 mm). In practical terms, the maximum scour depth remained below 0.1 cm (Table 6), corresponding to a scour reduction of over 98.5%, effectively representing complete scour suppression within the measurement uncertainty of the system (±1 mm), as illustrated in Figure 7.

Accordingly, the optimal configuration identified in this study is the double-layer, 5-row IPB system in the fully buried (flush) installation, which provided complete suppression of measurable local scour under the tested clear-water conditions. Table 5 compiles the maximum scour depth, the dimensionless scour depth ($d_{s\,\max}/B$), and the corresponding reduction efficiency for all experimental scenarios (all values at 12 h; baseline $d_{s,\max} = 6.8$ cm).

Error bars representing the combined experimental uncertainty of ±2 mm

(equivalent to approximately ±3% in scour reduction), derived from the repeatability analysis presented in Section 2.6, have been included in Figure 6. The differences in scour depth between placement levels for a given number of rows are consistently much larger than this uncertainty range, confirming that the observed trends are physically meaningful. For instance, with four rows, the scour depths for the on-bed, semi-buried, and buried configurations are 19, 15, and 11 mm, respectively. The 8 mm difference between the on-bed and buried placements is four times the ±2 mm uncertainty. Similarly, with one row, the difference between the on-bed (43 mm) and buried (31 mm) placements is 12 mm, which is six times the uncertainty. These results provide strong evidence that the performance hierarchy (buried > semi-buried > on-bed) is robust and not an artifact of experimental variability.

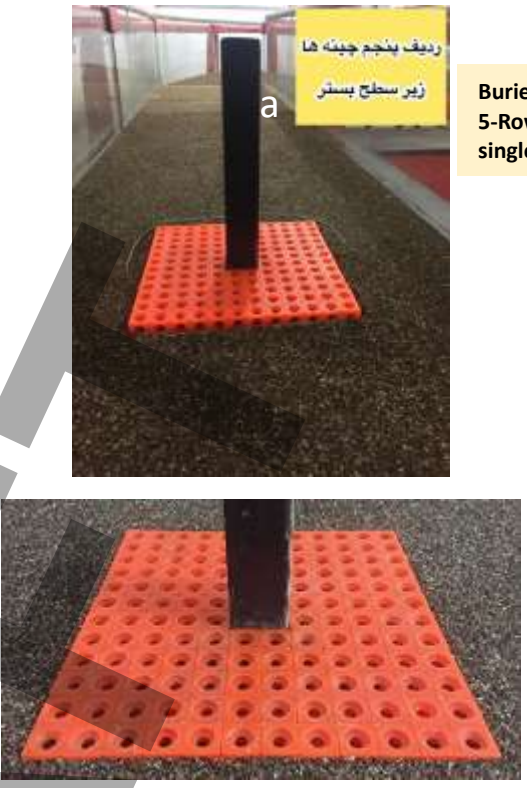

Fig. 7 Bed condition after the 5-row buried IPB tests: (a) single-layer; (b) double-layer (stacked).

Table 6 Summary of experimental results for maximum scour depth and reduction efficiency (all values at 12 hours; baseline = 6.8 cm)

Placement Level	Number of Rows	Maximum Scour Depth $d_{s\,max}$(cm)	Dimensionless Scour Depth $ds_{\,max}/B$	Scour Reduction (%)
Control (No Protection)	-	**6.8**	**1.7**	-
On-Bed	1	4.3	1	36.8
	2	2.6	0.6	61.8
	3	2.2	0.5	67.6
	4	1.9	0.4	72.1
Semi-Buried	1	3.9	0.9	42.6
	2	2.4	0.6	64.7
	3	2	0.5	70.6
	4	1.5	0.3	77.9
Buried	1	3.1	0.7	54.4
	2	2.2	0.5	67.6
	3	1.7	0.4	75
	4	1.1	0.2	83.8
	5(One Layer)	0.9	0.1	91.2
	5 (Double Layer)	**<0.1**	**<0.02**	**>98.5***

*No measurable scour was detected within the accuracy of the measurement system (±1 mm).

4. Discussion

The results of this study not only demonstrate the effectiveness of IPBs but also provide critical insights into the fundamental principles of scour protection. The discussion is organized into four parts: a direct comparison with existing countermeasures, an analysis of the governing hydraulic mechanisms, the implications of testing on a square pier, and the limitations of the current work.

4.1. Comparison with Previous Countermeasures

The performance of the novel Interlocking 3D Porous Blocks (IPBs) was evaluated by comparing the optimal configuration from this study with results from selected previous research on both flow-altering and bed-armoring countermeasures. The observation that no measurable scour occurred with the double-layer, 5-row buried IPB configuration represents a highly effective result.

To provide a direct, quantitative basis for this comparison, Table 7 summarizes the key experimental parameters and reported efficiencies from several key studies, including the present work. As shown, under clear-water conditions with a high flow intensity (U/Uc = 0.95), the optimal IPB arrangement achieved a scour reduction exceeding 98.5%.

.

Table 7 Quantitative Comparison of IPB Performance with Selected Previous Countermeasure Studies.

Study	Countermeasure	Pier Shape	d50 (mm)	y/B	B/d50	Duration (h)	Scour Reduction (%)
This Study	**IPB (Double-Layer, Buried)**	**Square**	**1.2**	**3.75**	**33.3**	**12**	**>98.5%**
Zarrati et al. (2004)	Collar	Rectangular	0.8	4	62.5	48	~70%
Kumar et al. (1999)	Slot	Circular	0.43	4	174	8	~30%
Melville & Hadfield (1999)	Sacrificial Piles	Circular	0.85	3	118	6	~56%
Lauchlan & Melville (2001)	Riprap	Circular	0.85	3	118	8	~80-100%*
Valela et al. (2022)	Articulating Concrete Blocks	Circular	0.88	3.7	85	21	>95%

A recent systematic review by Behera et al. (2026) noted that conventional flow-altering devices such as collars and slots typically yield scour reductions in the range of 40–80% in laboratory settings. The data in Table 7 supports this, showing typical efficiencies around ~70% for collars (Zarrati et al., 2004) and ~30% for slots (Kumar et al., 1999) under comparable conditions. While these devices can be effective, they often introduce vulnerabilities; for example, slots can become clogged with debris, and collars can be undermined if general bed degradation occurs. In stark contrast, the fully buried IPB system provides complete protection without protruding into the flow or compromising the pier's structural integrity. When compared to other bed-armoring systems, the IPB's performance is on par

with the most advanced solutions. While well-designed riprap can achieve near-100% protection, its stability relies on the gravitational weight of individual stones, making it susceptible to failure modes like shear failure and winnowing (Lauchlan & Melville, 2001). The IPBs' mechanical interlocking system, however, creates a coherent, monolithic mattress that resists these failure modes. The performance also aligns with that of other advanced armor units, such as Articulated Concrete Blocks (ACBs) and A-Jacks, which have similarly demonstrated near-complete scour reduction in laboratory studies (Valela et al., 2022; Zolghadr & Shafai-Bajestan, 2018).

The distinct advantage of the IPBs lies in their unique dual-function design. They not only provide a stable, interlocking armor layer but also feature a porous structure that dissipates the energy of the downflow and horseshoe vortex internally. This integrated mechanism, combining robust mechanical stability with hydraulic energy dissipation, positions the IPB system as a highly effective and promising solution for bridge foundation protection.

4.2. Mechanisms of Enhanced Performance

While direct measurements of the flow field within the block matrix were outside the scope of this study, the observed bed topography and established hydraulic principles allow for the inference of three synergistic mechanisms responsible for the superior performance of the buried IPB configuration.

1. Internal Energy Dissipation (The Porosity Effect): Unlike solid aprons (e.g., collars) that deflect the powerful down-flow jet, the IPBs absorb it. With a porosity of 25%, the interconnected lattice allows the high-energy flow to penetrate the block matrix. The kinetic energy of the impinging down-flow and horseshoe vortex is then dissipated through induced micro-turbulence within the block voids before reaching the erodible bed beneath. Future velocity measurements within the block matrix would be needed to confirm this mechanism.
2. Boundary Layer Stabilization and Form Drag Elimination: Placing armor units on the bed surface (On-Bed) creates an abrupt geometric change, inducing form drag and generating secondary turbulence at the mat's edge. This can inadvertently trigger scour at the periphery of the protection. By burying the blocks flush with the bed, the hydraulic smoothness of the approach flow is preserved. This design choice is observed to reduce edge-scour effects compared to on-bed placement, which is consistent with the superior performance of buried configurations in this study.
3. Winnowing Prevention (The Filtration Effect): A common failure mode for coarse armor layers is "winnowing," where underlying fine sediment is drawn out through the gaps. The dense, multi-layered (stacked) arrangement of IPBs creates a tortuous, three-dimensional path that significantly increases the pressure drop for any flow passing through it. This effectively "locks" the underlying sediment in place, preventing its erosion. This integrated design, where the IPB assembly functions as both the armor and the filter layer, is a key factor in its success.

4.3. Significance of Performance on Square Piers

It is noteworthy that the reported results were obtained using a square pier, which represents a "worst-case" hydraulic scenario due to pronounced flow separation at its sharp corners. Square piers induce more intense vortices and deeper scour than circular piers (Richardson & Davis, 1995). The high scour reduction achieved under these conditions suggests that the IPB system has a meaningful protective capacity. Performance on circular or streamlined piers may be achievable with

fewer rows or a single layer, potentially leading to more cost-effective designs, though this hypothesis requires experimental validation.

4.4. Limitations and Future Research Directions

While this study provides compelling evidence for the effectiveness of IPBs, its limitations highlight important avenues for future research.

- Scale Effects: The experiments were conducted at laboratory scale using a 40 mm pier and 20 mm blocks (Bb/B = 0.5). Scaling the results to field conditions requires careful consideration of block stability, interlocking performance under prototype forces, and potential changes in the relative importance of gravity, inertia, and viscous effects. Laboratory-scale results may not be directly transferable to field conditions without further validation.
- Live-Bed Conditions: All experiments were performed under clear-water conditions (U/Uc = 0.95). Under live-bed conditions, continuous sediment transport and deposition may alter the protective performance of IPBs. In particular, long-term sediment accumulation within the block pores could modify the hydraulic resistance and energy dissipation capacity of the system.
- Long-Term Durability: Issues such as clogging of pores by fine sediment, abrasion of block material, behavior under freeze-thaw cycles in cold climates, debris impact, and long-term structural settlement were not investigated. These factors are critical for evaluating the long-term field performance of IPBs.
- Installation Feasibility: Burying multi-layer IPB mats flush with the bed around existing bridge piers in active rivers with strong currents presents significant practical, logistical, and economic challenges. Field installation procedures and associated costs require dedicated investigation.
- Flow Measurements: No direct velocity, pressure, or turbulence measurements were obtained within or around the block matrix. Such data would be essential to confirm the proposed hydraulic mechanisms and to develop physics-based design guidelines.
- Repeatability: To verify experimental reproducibility, five randomly selected tests (six total runs including one double-repeated case) were conducted, yielding a maximum deviation of ±2 mm and a mean absolute deviation of 1.0 mm. While these results demonstrate good consistency, comprehensive replications for all configurations were not performed due to the large scope of the study. Future studies are recommended to include full replications to enable rigorous statistical uncertainty quantification.

Future research should include extended-duration flume tests, large-scale experiments, live-bed condition tests, field pilot installations, and advanced numerical modeling using porous media approaches (e.g., Brinkman–Forchheimer formulation) to provide deeper insights into the flow-structure interaction within the IPB matrix.

5. Conclusion

This experimental study investigated the efficacy of a novel bed-armoring countermeasure, Interlocking 3D Porous Blocks (IPBs), in mitigating local scour around square bridge piers under clear-water conditions. By systematically varying the placement level and areal extent of the protection, the following key conclusions can be drawn:

1. Critical Role of Placement Level: The vertical positioning of the protection mat proved to be a decisive factor. The buried configuration (flush with the bed) consistently outperformed on-bed and semi-buried placements. Whereas surface-mounted blocks reduced

scour, they also induced secondary turbulence and edge scour due to form drag. In contrast, buried blocks maintained hydraulic smoothness, functioning effectively as a sub-layer armor.

2. Efficiency and Areal Extent: The reduction in scour depth increased non-linearly with the number of block rows. For the buried configuration, increasing the protection extent from 1 row to 4 rows improved the scour reduction efficiency from 54% to 84%.
3. Suppression of Measurable Scour: The most significant finding was the exceptional performance of the double-layer, 5-row configuration buried flush with the bed. This arrangement suppressed local scour to a level below the instrumental detection limit (±1 mm), corresponding to a scour reduction efficiency exceeding 98.5%. Consequently, it maintained a virtually flatbed topography, even under the aggressive flow field generated by a square pier.
4. Superior Stability and Mechanism: Unlike loose riprap which is prone to shear failure and winnowing, the IPBs demonstrated superior stability due to their six-sided mechanical interlocking. The blocks formed a coherent, flexible mat that dissipated the kinetic energy of the scour-inducing vortices within their porous structure.

These laboratory results suggest that IPBs are a highly promising alternative to traditional countermeasures. However, it is crucial to recognize that these conclusions are based on the specific conditions tested. Field-scale validation under a wider range of hydraulic and environmental conditions is essential before practical implementation can be recommended. Future research, as outlined in the discussion, is needed to validate these findings and assess long-term field performance.

References:

Behera, R.K., Padhi, E., & Singhal, G.D. (2026). Recent trends in local scour countermeasure for bridge piers. Engineering Science and Technology, an International Journal, 77, 102367**.**

Chiew, Y. M. (2004). Local scour and riprap stability at bridge piers in a degrading channel. *Journal of Hydraulic Engineering, 130*(3), 218–226.

Chiew, Y. M., & Melville, B. W. (1987). Local scour around bridge piers. *Journal of Hydraulic Research, 25*(1), 15–26.

Kumar, V., Ranga Raju, K. G., & Vittal, N. (1999). Reduction of local scour around bridge pier using slots and collar. *Journal of Hydraulic Engineering, 125*(12), 1302-1305.

Lagasse, P. F., Schall, J. D., Johnson, F., Richardson, E. V., & Chang, F. (1995). *Stream stability at highway structures* (2nd ed., HEC-20, Publication No. FHWA-IP-90-014). Federal Highway Administration.

Lauchlan, C. S., & Melville, B. W. (2001). Riprap protection at bridge piers. *Journal of Hydraulic Engineering, 127*(5), 412–418.

Macky, G. H. (1990). *Survey of roading expenditure due to scour* (Publication No. 20). DSIR Hydrology Centre.

Melville, B. W., & Coleman, S. E. (2000). *Bridge scour*. Water Resources Publications.

Melville, B. W., & Hadfield, A. C. (1999). Use of sacrificial piles as pier scour countermeasures. *Journal of Hydraulic Engineering, 125*(11), 1221–1224.

Melville, B. W., & Sutherland, A. J. (1988). Design method for local scour at bridge piers. *Journal of Hydraulic Engineering, 114*(10), 1210–1226.

Miller, W. (2003). *Model for the time rate of local sediment scour at a cylindrical structure* [Doctoral dissertation, University of Florida].

Moncada-M, A. T., Aguirre-Pe, J., Bolivar, J. C., & Flores, E. J. (2009). Scour protection of circular bridge piers with collars and slots. *Journal of Hydraulic Research, 47*(1), 119–126.

Raudkivi, A. J., & Ettema, R. (1983). Clear-water scour at cylindrical piers. *Journal of Hydraulic Engineering, 109*(3), 339–350.

Richardson, E. V., & Davis, S. R. (1995). *Evaluating scour at bridges* (3rd ed., HEC-18, Publication No. FHWA-IP-90-017). Federal Highway Administration.

Tafarojnoruz, A., Gaudio, R., & Calomino, F. (2012). Evaluation of flow-altering countermeasures against bridge pier scour. *Journal of Hydraulic Engineering, 138*(3), 297–305.

Valela, C., Whittaker, C. N., Rennie, C. D., Nistor, I., & Melville, B. W. (2022). Novel riprap structure for improved bridge pier scour protection. *Journal of Hydraulic Engineering*, *148*(3), 04022002.

Zarrati, A. R., Gholami, H., & Mashahir, M. B. (2004). Application of collar to control scouring around rectangular bridge piers. *Journal of Hydraulic Research, 42*(1), 97–103.

Zolghadr, M., & Shafai-Bajestan, M. (2018). Scour around A-Jacks armor units. *International Journal of River Basin Management, 16*(2), 221–228.